PROCEEDINGS OF SCIENCE

Global characteristics of the proton-lead collisions in ATLAS

Mauro Villa*
on behalf of the ATLAS Collaboration
INFN Bologna and University of Bologna
E-mail: mauro.villa@unibo.it

The ATLAS experiment has studied the centrality dependence of global event characteristics in proton-lead collisions at $\sqrt{s_{\rm NN}} = 5.02$ TeV. A total integrated luminosity of 30 nb^{-1} was collected during LHC proton-lead runs in the fall of 2012 and winter of 2013.

Two analyses on two and multi-particle correlations have been performed using different techniques on the first pilot run of proton-lead collisions (with integrated luminosity $\mathscr{L} \approx 1\ \mu$b^{-1}) taken with a minimum bias trigger. In both analyses, the centrality of proton-lead collisions was characterized using the total transverse energy ($\sum E_{\rm T}^{\rm Pb}$) measured in the ATLAS forward calorimeter on the Pb-going side of the detector.

In the first analysis, two-particle correlations in relative azimuthal angle ($\Delta\phi$) and pseudorapidity ($\Delta\eta$) are measured. The correlation function, constructed from charged particle pairs, shows a long-range ($2 < |\Delta\eta| < 5$) near-side ($\Delta\phi \approx 0$) correlation that grows rapidly with increasing $\sum E_{\rm T}^{\rm Pb}$. After subtracting the recoil correlations due to dijets and low $p_{\rm T}$ resonance decays, a long-range ($2 < |\Delta\eta| < 5$) away-side ($\Delta\phi \approx \pi$) correlation is found with characteristics matching the near-side correlation in magnitude, shape, $p_{\rm T}$ and $\sum E_{\rm T}^{\rm Pb}$ dependence. The Fourier analysis of the $\Delta\phi$ correlation with the subtracted recoil component allowed to extract the elliptic flow coefficients $v_2(p_{\rm T})$ as a function of $p_{\rm T}$ of one of the particles forming the pair.

In a second analysis on the same data, the elliptic flow coefficients have been extracted with the cumulant method for two particles and four particles. Results are shown as a function of $p_{\rm T}$ and $\sum E_{\rm T}^{\rm Pb}$. The elliptic flow measurements on four particles, $v_2\{4\}$, sensitive to flow effects only, and on two particle correlations (recoil subtracted), $v_2\{2{\rm PC}\}$, are in good agreement. The main results are compared with the few theoretical models available for p+Pb interactions in the TeV energy regime.

The 2013 European Physical Society Conference on High Energy Physics (EPSHep 2013)
18-24 July 2013
Stockholm, Sweden

*Speaker.

ATL-PHYS-PROC-2013-244
27 September 2013

PoS(EPS-HEP 2013)199

To have a complete picture of the hadronic interactions at LHC, in addition to the studies of pp and Pb+Pb collisions, the investigation of p+Pb collisions is considered to be mandatory [1]. From one side, p+Pb collisions are of utter importance in their own since at high energies they allow to explore the QCD at high parton densities and offer a unique opportunity to study the saturation of the nuclear parton distributions functions. From another side they provide baseline measurements for Pb+Pb studies. The unambiguous interpretation of Pb+Pb data is difficult due to the simultaneous presence of the initial state effects and final state effects, the latter used to characterize the properties of the hot and dense QCD matter produced in Pb+Pb collisions. The study of p+Pb collisions is crucial to disentangle the initial state effects from those due to the creation of the hot nuclear matter.

For these reasons, a large sample of p+Pb collisions, having a total integrated luminosity $\mathscr{L} \approx 30$ nb^{-1}, has been taken this year at $\sqrt{s_{\rm NN}} = 5.02$ TeV with the ATLAS detector [2]. In this report, we present results [3, 4] obtained with the first pilot run in which p+Pb collisions were collected using a minimum bias trigger for a total integrated luminosity of $\mathscr{L} \approx 1\,\mu$b^{-1}. Three sub-detectors were mainly involved in the event selection and reconstruction: the MBTS scintillators for the minimum bias trigger and event cleaning, the Inner Detector for the charged track reconstruction and the forward calorimeter (FCal) on the lead-going side for the study of the activity of the p+Pb interaction.

The reconstructed events are cleaned for the non-collision background, photointeractions and pile-up interactions. Only events with a single well identified primary vertex in a $|z_{\rm vtx}| < 150$ mm fiducial region are selected for further analysis.

All the analyses of p+Pb collisions are performed in different classes of events to take into account the reaction kinematics. For an extimation of it, it is possible to use both the number of reconstructed charged tracks ($N_{\rm ch}^{\rm rec}$) or the transverse energy ($\sum E_{\rm T}^{\rm Pb}$) measured by the Pb-going side of the FCal module. On the left of Fig. 1, a scatter plot of these two quantities shows that they are strongly correlated even if the η acceptances of the Inner Detector ($|\eta| < 2.5$) and of FCal ($3.1 < |\eta| < 4.9$) do not overlap at all. To avoid any auto-correlation bias in the track selection, the event classification is done using the transverse energy. On the right of Fig. 1 the $\sum E_{\rm T}^{\rm Pb}$ is shown

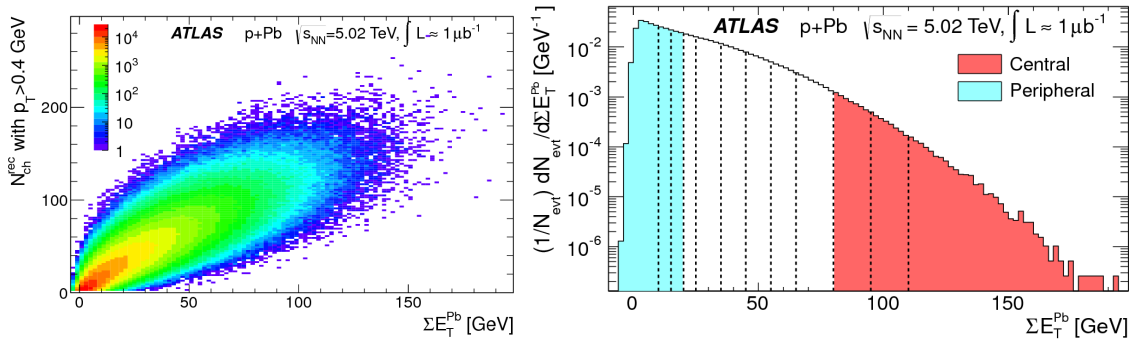

Figure 1: Left. Scatter plot of the number of charged tracks found in the Inner Detector vs the transverse energy ($\sum E_{\rm T}^{\rm Pb}$) measured in FCal for minimum-bias p+Pb events. Right. Distribution of $\sum E_{\rm T}^{\rm Pb}$ for the same event sample [3]. Vertical lines define the boundaries of the event activity classes. Shaded bands refer to the peripheral and central intervals having $\sum E_{\rm T}^{\rm Pb} < 20$ GeV (light blue) and $\sum E_{\rm T}^{\rm Pb} > 80$ GeV (red), respectively.

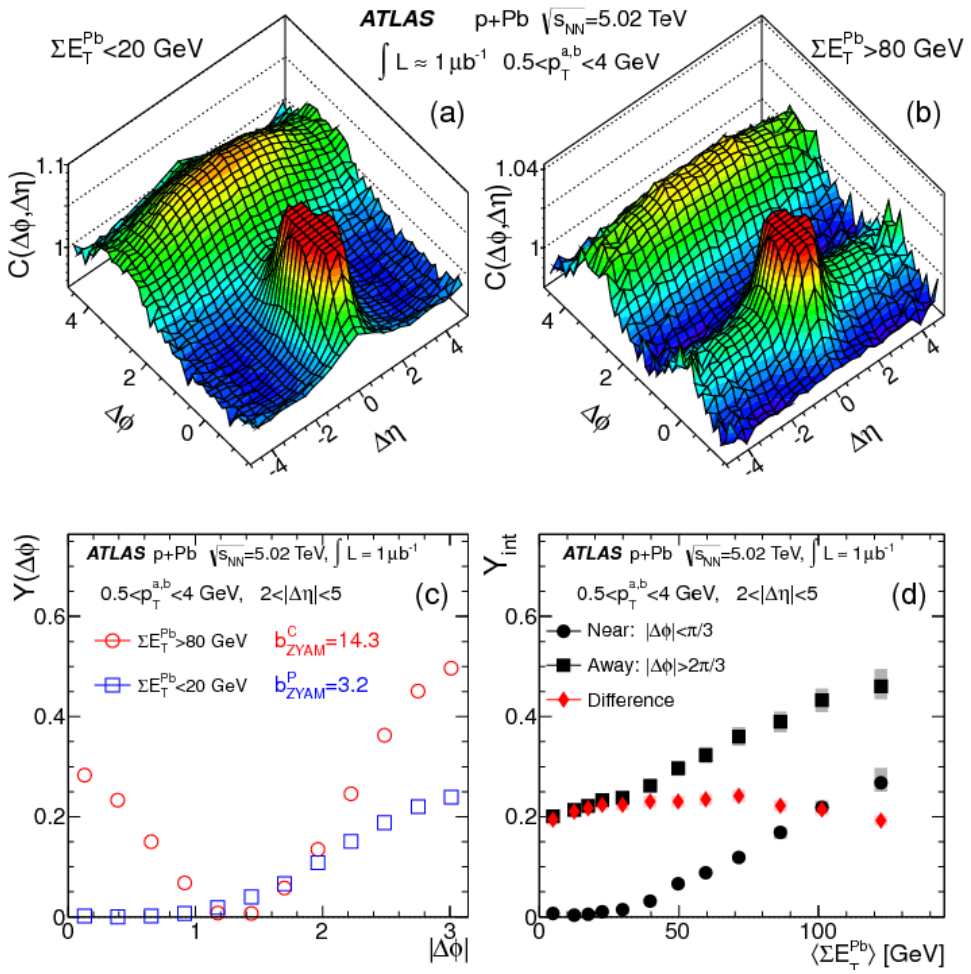

Figure 2: Two-dimensional correlation functions [3] for (a) peripheral events and (b) central events, both with a truncated maximum to suppress the large correlation at $(\Delta\eta, \Delta\phi) = (0,0)$; (c) the per-trigger yield distribution ($Y(\Delta\phi)$) with indicated pedestal levels for peripheral ($b^{\mathrm{P}}_{\mathrm{ZYAM}}$) and central ($b^{\mathrm{C}}_{\mathrm{ZYAM}}$) events, and (d) integrated per-trigger yield Y^{int} as function of $\sum E_{\mathrm{T}}^{\mathrm{Pb}}$ for pairs with $2 < |\Delta\eta| < 5$. The shaded boxes represent the systematic uncertainties, and the statistical uncertainties are smaller than the symbols.

together with vertical bands that define separated activity classes. The two extreme colored bands contain the $\sum E_{\mathrm{T}}^{\mathrm{Pb}} > 80$ GeV events (top 2% of events) that defines the *central* collision class and the $\sum E_{\mathrm{T}}^{\mathrm{Pb}} < 20$ GeV events (lowest 52%) that defines the *peripheral* collision class.

In the first analysis performed on the p+Pb sample [3], we studied the two particle correlations (2PC) observing how the difference in azimuthal angle ($\Delta\phi$) and in pseudorapidity ($\Delta\eta$) between two tracks is distributed on all pairs of tracks in an event and on all events. The two-dimensional distribution $S(\Delta\phi, \Delta\eta)$ obtained in this way is modulated by correlations and acceptance effects. To remove the latter ones, a background correlation-free distribution $B(\Delta\phi, \Delta\eta)$ is built with a mixed event technique: we pair tracks from different events belonging to the same centrality class. The ratio $C(\Delta\phi, \Delta\eta) = S/B$ is free from acceptance effects and contains the correlation information we search for. In Fig. 2 (a), the $C(\Delta\phi, \Delta\eta)$ function is shown for peripheral events. There is a clear correlation at $\Delta\phi = 0, \Delta\eta = 0$ due to charged tracks belonging to the same jet or coming from high

p_{T} resonances, and there is a weaker correlation at $|\Delta\phi| \approx \pi$ due to particles recoiling against jets (the so-called recoil correlation). For central events (Fig. 2 (b)), there is an interesting long-range correlation in $\Delta\eta$ at $\Delta\phi = 0$ and a *broader* recoil correlation. These two effects are the so called near-side ($\Delta\phi \approx 0$) and away side ($|\Delta\phi| \approx \pi$) ridge respectively. The intensities of these long range correlations in p+Pb interactions are qualitatively similar to what has been observed by CMS [5, 6], and ALICE [7] in a reduced $|\Delta\eta|$ range. Remarkably, the near side long range correlation has been observed also in high track multiplicity pp events [8].

To show better these long range correlations we restricted the analysis to particle pairs with $2 < |\Delta\eta| < 5$ removing in this way the largest part of the trivial near side and away side correlations. The strength of the long-range correlation is quantified by the so called per-trigger yield function $Y(|\Delta\phi|)$, that measures the correlation between two particles in the restricted $\Delta\eta$ range at a given $|\Delta\phi|$. Its minimum value is fixed to zero so that positive correlations are clearer. This quantity is shown on the bottom left of Fig. 2 for peripheral and central events: while in the peripheral events there is no correlation on the near side and there is a recoil correlation on the away side, in the central event class the near side and the away side correlations are stronger. By integrating the $Y(|\Delta\phi|)$ in the near ($|\Delta\phi| < \pi/3$) and away ($2\pi/3 < |\Delta\phi| < \pi$) regions, we obtain the so-called integrated per-trigger yield Y_{int}, which shows (bottom right of Fig. 2) that apart from the constant term of the recoil correlation, the near side and the away side ridges increase with centrality ($\sum E_{\mathrm{T}}^{\mathrm{Pb}}$)

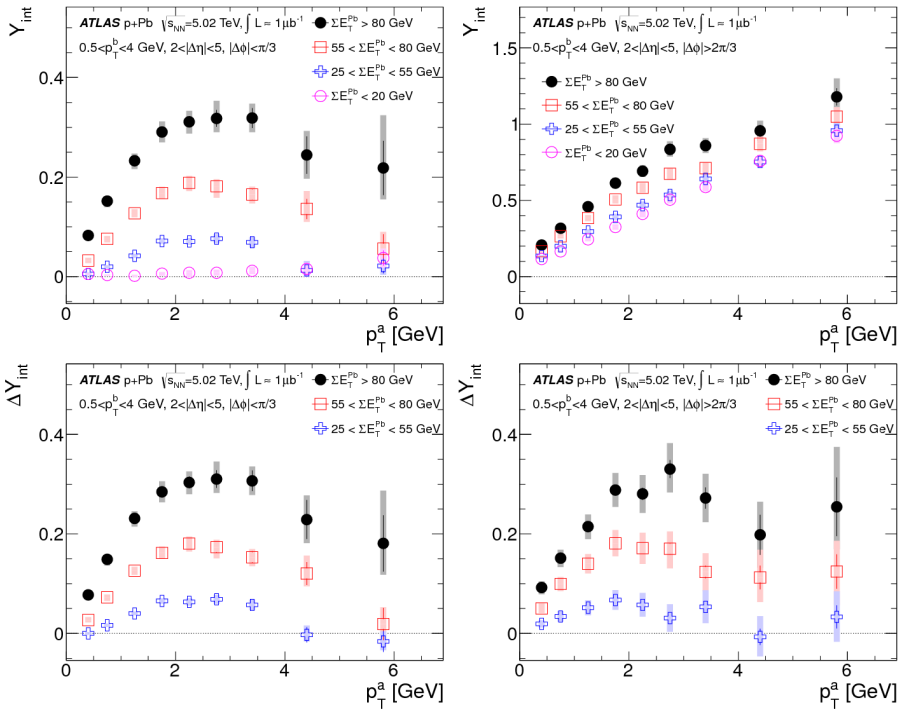

Figure 3: Integrated per-trigger yields Y_{int} vs p_{T}^{a} for $0.5 < p_{\mathrm{T}}^{b} < 4$ GeV in various $\sum E_{\mathrm{T}}^{\mathrm{Pb}}$ event classes on the near-side (top left) and away-side (top right). The bottom panels show the difference of the yield from that in the $\sum E_{\mathrm{T}}^{\mathrm{Pb}} < 20$ GeV event class. The error bars and shaded boxes represent the statistical and systematic uncertainties, respectively.

in the same way. In Fig. 3, $Y_{\rm int}$ is shown as a function of $p_{\rm T}$ of one of the particles for different centrality classes. The lower part of the figure shows that, after subtraction of the integrated per-trigger yield of the most peripheral class, the $p_{\rm T}$ behaviour of the near (left) and away (right) side is the same in all centrality classes.

Another differential analysis of the per-trigger yield as a function of $p_{\rm T}$ showed that in all $p_{\rm T}$ ranges (in $0.3 < p_{\rm T} < 5$ GeV) the near and away ridges have the same intensity (although varying with $p_{\rm T}$). The per-trigger yield difference (ΔY) between central and peripheral events contains a dominant behavior on $\Delta\phi$ that varies as $\cos 2|\Delta\phi|$ (see Fig. 4). This dependence can be interpreted as an evidence for collective phenomena in p+Pb collisions. Nevertheless there is also a different interpretation: a Color Glass Condensate model [9] is able to reproduce remarkably well both the intensity of the per-trigger yield for peripheral and for central events and their $p_{\rm T}$ dependence (see [9] for details). In this case, the observed effect is interpreted as an initial state effect: the saturation of the gluon parton distribution in the nucleus.

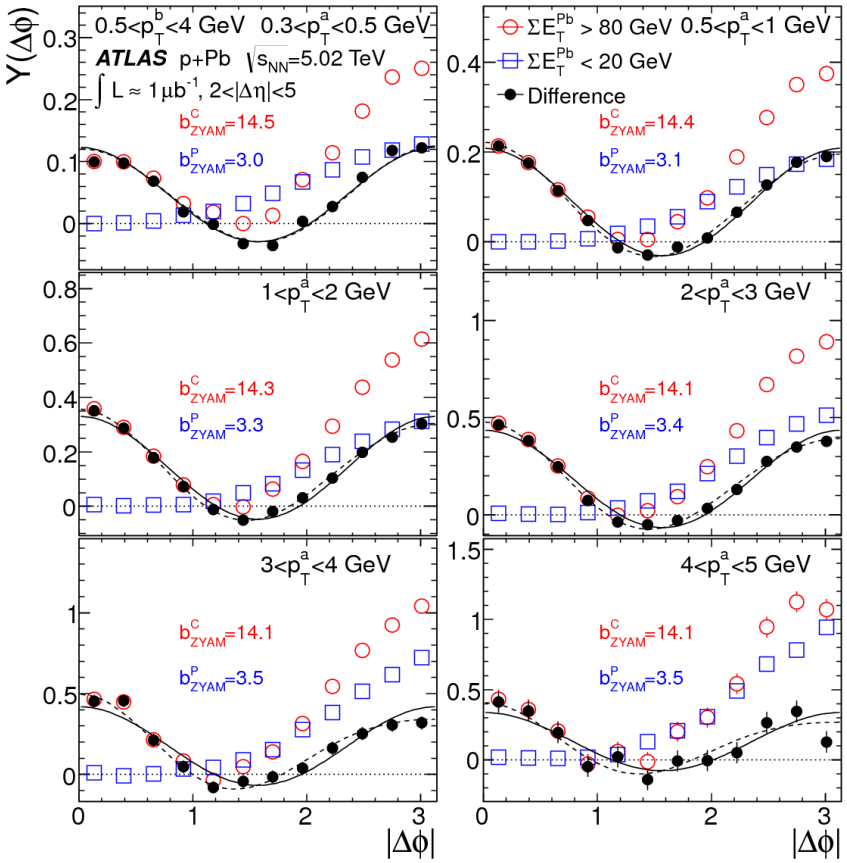

Figure 4: Distributions of per-trigger yield in the peripheral and the central event activity classes and their differences (solid symbols), for different ranges of $p_{\rm T}^a$ and $0.5 < p_{\rm T}^b < 4$ GeV, together with functions $a_0 + 2a_2\cos 2\Delta\phi$ (solid line) and $a_0 + 2a_2\cos 2\Delta\phi + 2a_3\cos 3\Delta\phi$ (dashed line) obtained via a Fourier decomposition (see [3] for details).

The intensity of the $\cos 2|\Delta\phi|$ modulation of ΔY is related to the elliptic flow coefficient v_2. By studying the intensity in different centrality classes and for different ranges of $p_{\rm T}$, the $v_2(p_{\rm T})$ coefficients are extracted and shown as red squares in Fig. 5. To investigate further the elliptic

flow, a different and complementary analysis has been performed [4] on the same pilot run data. The elliptic flow can be evaluated with a variety of methods [10, 11, 12, 13] and can be extracted with different combinations of particles in an event. In this analysis [4] the so called *cumulant method* [10, 11, 12] has been applied to extract the v_2 and $v_2(p_T)$ coefficients from two and four particle cumulants, $v_2\{2\}$ and $v_2\{4\}$. The main advantage of the cumulant method is that it provides two partially independent estimations of v_2 with different systematics: in particular the two track elliptic flow coefficient, $v_2\{2\}$, is sensitive to non-flow contributions like jets or decays of high p_T resonances, while the four particle coefficient, $v_2\{4\}$ is not sensitive to two-particle correlations generated by these contributions, but it has usually larger uncertainties. The full description of the analysis can be found in [4]. Here only the final results separated in four centrality classes and as a function of p_T are discussed and shown in Fig. 5. The results of the four particle cumulants, that are sensitive to flow effects only, are shown in the figure with the stars and are always compatible with the 2PC method accounting for charged particle pairs with $2 < |\Delta\eta| < 5$ [3]. The two particle cumulant method, instead, being sensitive also to non flow effects provides systematically an over estimation of the elliptic flow. The p_T dependence of both $v_2\{4\}$ and $v_2\{2PC\}$ in p+Pb collisions resembles quite closely what has been measured for v_2 in Pb+Pb collisions at $\sqrt{s_{NN}} = 2.76\,\text{TeV}$ [14, 15]. In Fig. 6 the elliptic flow coefficients are shown integrated in p_T as a function of $\sum E_T^{Pb}$. The first estimations [16] of the elliptic flow based on viscous hydrodynamics tuned on Pb+Pb data but performed for p+Pb at $\sqrt{s_{NN}} = 5\,\text{TeV}$ are in a remarkable agreement with our data. This agreement is an indication towards the importance of final state effects in p+Pb collisions.

In conclusions, from the first p+Pb data at 5 TeV, ATLAS has observed the near side and the away side correlation for an extended $\Delta\eta$ range ($2 < |\Delta\eta| < 5$) for the first time [3]. The correlation has been studied as a function of the event activity and p_T. The elliptic flow coefficients have been extracted with several methods: the two particle correlation [3] and the cumulant method for the two and four particle combinations [4]. The different methods allow an internal consistency check of the data and the estimation of non flow contributions which are found to be significant in $v_2\{2\}$. The data have been compared with theoretical models [9, 16] able to reproduce remarkably well

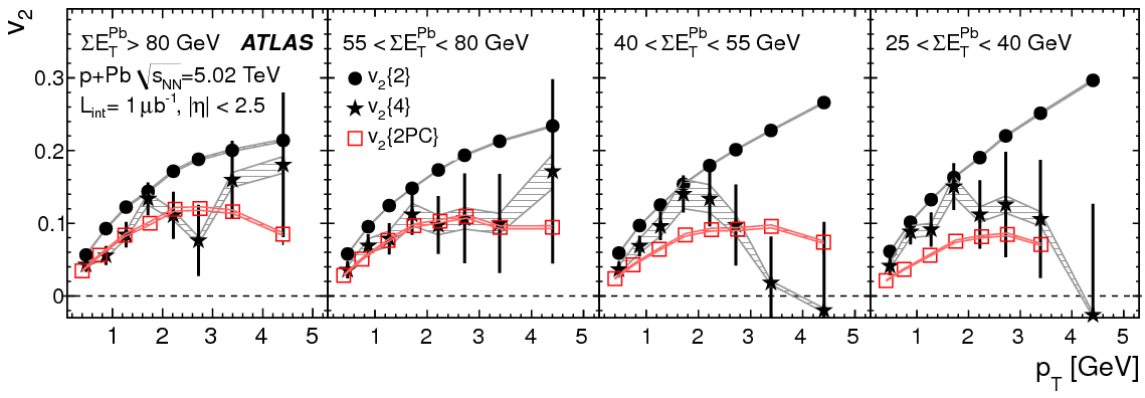

Figure 5: The elliptic flow coefficients $v_2(p_T)$ derived from the two-particle correlation analysis (2PC) as a function of p_T in four different activity intervals are shown by red squares [4]. The v_2 calculated with the cumulant method are shown for two particles ($v_2\{2\}$, circles) and four particles ($v_2\{4\}$, stars). Bars denote statistical errors; systematic uncertainties are shown as shaded bands.

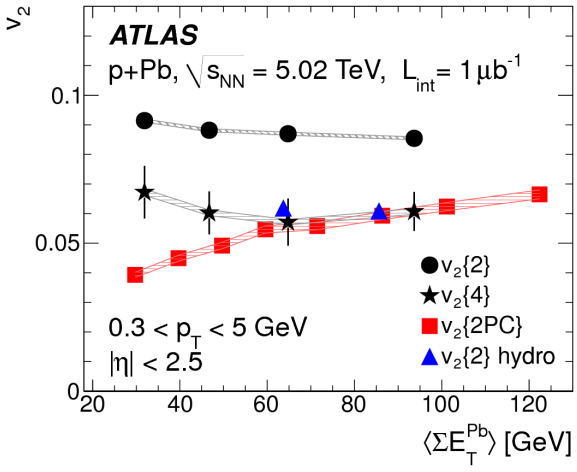

Figure 6: The elliptic flow coefficient v_2, integrated over p_{T} and η, calculated with two- and four-particle cumulants (circles and stars, respectively), as a function of $\sum E_{\mathrm{T}}^{\mathrm{Pb}}$ [4]. Systematic uncertainties are shown as shaded bands. Also shown is $v_2\{2\mathrm{PC}\}$ (red squares) and predictions [16] (triangles) from an hydrodynamic model for the same selection of charged particles as in the data.

the observed features, from the ridges to the v_2, despite their different approaches to the p+Pb dynamics.

References

[1] C. Salgado *et al.*, J. Phys. **G39** (2012) 015010 [arXiv:1105.3919 hep-ph].

[2] ATLAS Collaboration, JINST **3** (2008) S08003.

[3] ATLAS Collaboration, Phys. Rev. Lett. **110** (2013) 182302 [arXiv:1212.5198 hep-ex].

[4] ATLAS Collaboration, Phys. Lett. **B 725** (2013) 60 [arXiv:1303.2084 hep-ex].

[5] CMS Collaboration, Phys. Lett. **B 718** (2013) 795 [arXiv:1210.5482 nucl-ex].

[6] CMS Collaboration, Phys. Lett. **B 724** (2013) 213 [arXiv:1305.0609 nucl-ex].

[7] ALICE Collaboration, Phys. Lett. **B 719** (2013) 29 [arXiv:1212.2001 nucl-ex].

[8] CMS Collaboration, J. HEP **09** (2010) 091 [arXiv:1009.4122 hep-ex].

[9] K. Dusling and R. Venugopalan, Phys. Rev. **D 87** (2013) 094034 [arXiv:1302.7018 hep-ph].

[10] A. M. Poskanzer, S. A. Voloshin, Phys. Rev. **C 58** (1998) 1671 [arXiv:9805001 nucl-ex].

[11] N. Borghini, P. M. Dinh, J. -Y. Ollitrault, Phys. Rev. **C 63** (2001) 054906 [arXiv:0007063 nucl-th].

[12] N. Borghini, P. M. Dinh, J. -Y. Ollitrault, Phys. Rev. **C 64** (2001) 054901 [arXiv:0105040 nucl-th].

[13] A. Bilandzic, R. Snellings, S. Voloshin, Phys. Rev. **C 83** (2011) 044913 [arXiv:1010.0233].

[14] ATLAS Collaboration, Phys. Rev. **C 86** (2012) 014907 [arXiv:1203.3087 hep-ex].

[15] ATLAS Collaboration, Phys. Lett. **B 707** (2012) 330 [arXiv:1108.6018 hep-ex].

[16] P. Bożek,W. Broniowski, Phys. Lett. **B 718** (2013) 1557 [arXiv:1211.0845 nucl-th].